Control of Molecular Aggregations by Doping in Mesophases: Transformation of Smectic C Phases to Smectic C_A Phases by Addition of Long Bent-Core Molecules Possessing a Central Strong Dipole

Keiki Kishikawa,*,† Naoki Muramatsu,† Shigeo Kohmoto,† Kentaro Yamaguchi,‡ and Makoto Yamamoto†

Department of Materials Technology, Faculty of Engineering, and Chemical Analysis Center, Chiba University, 1-33 Yayoi-cho, Inage-ku, Chiba 263-8522, Japan

Received February 9, 2003. Revised Manuscript Received June 24, 2003

Compounds **1**−**3**, each possessing a long bent-rod shape and a central large dipole, were designed and synthesized as dopants which transform liquid-crystal smectic C phases to smectic C_A phases. The properties and the layer structures of the dopant molecules in the mesophases were investigated by polarized light microscopy, differential scanning calorimetry (DSC), and X-ray diffraction (XRD). Induction of smectic C_A phases from the smectic C phases of compounds **4**−**7** was performed by doping with a small amount of dopants **1**−**3**. In particular, even 1 wt % (0.5 mol %) of **3c** was enough to convert the Sm-*C* phase into the Sm-C_A phase in the case of **4**. In addition, matching in the core-lengths was important for the induction. Further, importance of the central dipole was also confirmed by replacement of the CF_3 groups of compound **1** with CH_3 or H.

Introduction

Control of molecular aggregations by doping is one of the most effective methods to organize molecules in mesophases, and is also important to induce novel and excellent properties in materials.[1,2] In liquid-crystal smectic C (Sm-*C*) phases (Scheme 1a), helical superstructures of chiral Sm-*C* (Sm-*C**) phases have been induced by doping with a chiral dopant.[3−6] The helicities originate in the small rotational angle of the tilt direction on passing from one layer to the next. The more effective the dopant is, the larger rotational angle is expected. On the other hand, a smectic C_A (Sm-C_A) phase (Scheme 1b) is known as one of the Sm-*C* phases in which the tilt direction is rotated by the ultimate rotational angle, 180° (Scheme 1b). Accordingly, it seems possible that a Sm-*C* phase can be converted to a Sm-C_A phase by doping. However, methodology to induce a Sm-C_A phase by doping has not yet been established.

Scheme 1. Schematic Side Views of Layer Structures: (a) Smectic C Phase and (b) Smectic C_A Phase

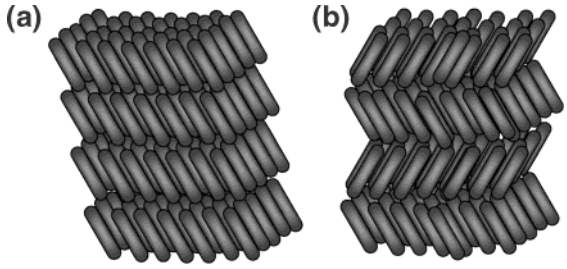

Chiral Sm-C_A (Sm-C_A*) phases have been thought to have a high potential for realizing the next-generation liquid crystal displays with rapid switching and high quality since the discovery of Sm-C_A phases in 1989.[7] Despite various studies after their discovery,[8,9] it has not yet been clarified what kind of molecules generate this phase nor how the layer structure is generated. The

* To whom correspondence should be addressed (kishikawa@faculty.chiba-u.jp).
† Department of Materials Technology, Faculty of Engineering.
‡ Chemical Analysis Center.

(1) (a) Gregg, B. A.; Cormier, R. A. *J. Am. Chem. Soc.* **2001**, *123*, 7959. (b) Wiederrecht, G. P.; Yoon, B. A.; Svec, W. A.; Wasielewski, M. R. *J. Am. Chem. Soc.* **1997**, *119*, 3358. (c) Jana, T.; Chatterrjee, J.; Nandi, A. K. *Langmuir* **2002**, *18*, 5720. (d) Williams, V. E.; Lemieux, R. P. *J. Am. Chem. Soc.* **1998**, *120*, 11311.

(2) (a) Thisayukta, J.; Niwano, H.; Takezoe, H.; Watanabe, J. *J. Am. Chem. Soc.* **2002**, *124*, 3354. (b) di Matto, A.; Todd, S. M.; Gottarelli, G.; Solladié, G.; Williams, V. E.; Lemieux, R. P.; Ferrarini, A.; Spada, G. P. *J. Am. Chem. Soc.* **2001**, *123*, 7842. (c) Yamaguchi, T.; Inagawa, T.; Nakazumi, H.; Irie, S.; Irie, M. *Chem. Mater.* **2000**, *12*, 869. (d) Green, M. M.; Zanella, S.; Gu, H.; Takahiro, S.; Gottarelli, G.; Jha, S. K.; Spada, G. P.; Schoevaars, A. M.; Feringa, B.; Teramoto, A. *J. Am. Chem. Soc.* **1998**, *120*, 9810. (e) Yarovoy, Y. K.; Labes, M. M. *J. Am. Chem. Soc.* **1997**, *119*, 12109. (f) Rosini, C.; Spada, G. P.; Proni, G.; Masiero, S.; Scamuzzi, S. *J. Am. Chem. Soc.* **1997**, *119*, 506. (g) Radley, K.; McLay, N.; Gicquel, K. *J. Phys. Chem. B* **1997**, *101*, 7404. (h) Radley, K.; Lilly, G. J. *Langmuir* **1997**, *13*, 3575.

(3) Sasaki, T.; Katsuragi, A.; Ohno, K. *J. Phys. Chem. B* **2002**, *106*, 2520.

(4) Thisayukta, J.; Nakayama, Y.; Kawachi, S.; Takezoe, H.; Watanabe, J. *J. Am. Chem. Soc.* **2000**, *122*, 7441.

(5) (a) Maly, K. E.; Wand, M. D.; Lemieux, R. P. *J. Am. Chem. Soc.* **2002**, *124*, 7898. (b) Dinescu, L.; Lemieux, R. P. *J. Am. Chem. Soc.* **1997**, *119*, 8111.

(6) (a) Vizitiu, D.; Lazar, C.; Halden, B. J.; Lemieux, R. P. *J. Am. Chem. Soc.* **1999**, *121*, 8229. (b) Lazer, C.; Wand, M. D.; Lemieux, R. P. *J. Am. Chem. Soc.* **2000**, *122*, 12586. (c) Yang, K.; Campbell, B.; Birch, G.; Williams, V. E.; Lemieux, R. P. *J. Am. Chem. Soc.* **1996**, *118*, 9557. (d) Lemieux, R. P. *Acc. Chem. Res.* **2001**, *34*, 845. (e) Vizitiu, D.; Lazar, C.; Radke, J. P.; Hartley, C. S.; Glaser, M. A.; Lemieux, R. P. *Chem. Mater.* **2001**, *13*, 1692.

(7) Chandani, A. D. L.; Gorecka, E.; Ouchi, Y.; Takezoe, H.; Fukuda, A. *Jpn. J. Appl. Phys.* **1989**, *28*, L1265.

10.1021/cm0340476 CCC: $25.00
Published on Web 07/30/2003

Scheme 2. Dopant Molecules 1−3

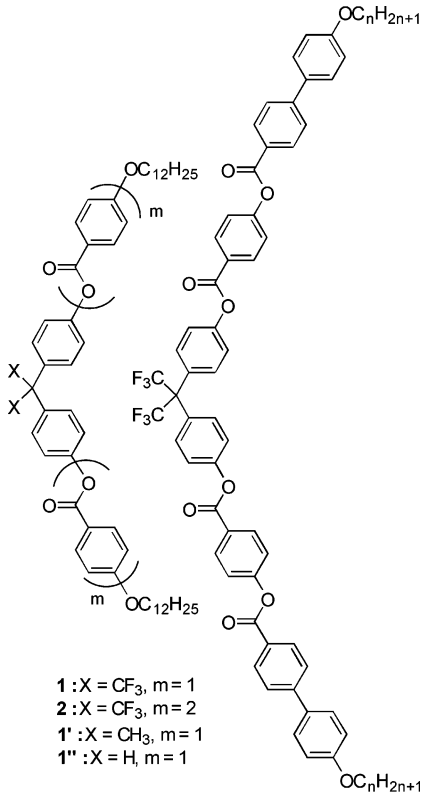

molecular designs have been performed empirically, which caused limitations in their molecular structures. Accordingly, the following factors, three rings, one ester linkage, one branched (chiral) terminal chain, and one *n*-alkyl terminal chain,[9a] have been considered to be essential for generation of Sm-C_A phases. A breakthrough has been eagerly awaited to realize an easy and reliable method to induce Sm-C_A phases.

In this paper, we designed and synthesized compounds **1**−**3** (Scheme 2) as the dopants to transform Sm-*C* phases to Sm-C_A phases. The properties and the layer structures of the dopant molecules were investigated by polarized light microscopy, differential scanning calorimetry (DSC), and X-ray diffraction (XRD). Conversion of the Sm-*C* phases of compounds **4**−**7** to Sm-C_A phases was performed by doping with **1**−**3**. We confirmed that even 1 wt % (0.5 mol %) of **3c** was enough to change the Sm-*C* phase into the Sm-C_A phase in the case of **4**.

Recently, Gorecka et al. has reported an example of induction of a Sm-C_A* phase from a Sm-*C** phase by doping.[10] They concluded that the twisting power of the Sm-*C** phase was increased by doping with banana-shaped molecules possessing a chiral conformation with 0.1−2 wt % contents of the dopant, to induce the Sm-C_A* phase. To argue their assumption, they also cited an unpublished example in which doping with banana-shaped molecules caused a shift of the transition temperature between the Sm-C_A* and Sm-*C** phases of 4-(1-methylheptyloxycarbonyl)phenyl 4′-octyloxybiphenyl-4-carboxylate) (MHPOBC).[11]

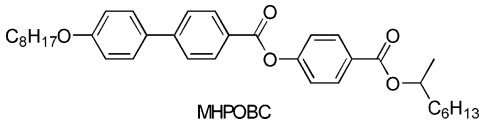

MHPOBC

Those examples were explained as a phenomenon caused by the chiral conformation of the banana-shaped molecules in the chiral environment. Another example also showed that the achiral dopant (1,1-dimethylheptyl 4-(4′-octyloxy-biphenyl-4-carbonyloxy)benzoate) induced a Sm-C_A from a Sm-*C* phase with the range over 20 wt % of it.[12] The phenomenon was explained by steric effect of the molecules at the layer boundaries. Further, induction of a biaxial bilayer smectic A (Sm-*A*) phase from a bilayer Sm-*A* phase was reported by doping with bent-core molecules with 4−13% of the contents.[13] In a computational study using a Monte Carlo method, induction of a Sm-C_A phase from a Sm-*A* phase by doping with bent-core molecules was simulated.[14] These recent reports have indicated a high possibility for induction of Sm-C_A phases from Sm-*C* phases by doping with bent-core molecules. However, to the best of our knowledge, an effective and generalized method to induce a Sm-C_A phase from a Sm-*C* phase by doping has not been realized.

To explain generation of Sm-C_A* phases in chiral liquid crystalline compounds possessing an asymmetric carbon atom at the terminal chain, the following two models have been postulated: (1) pairing of molecules at the boundary of the two neighboring layers using dipole−dipole interaction between the polar substituents at their asymmetric carbon atoms;[15] and (2) cancellation of macroscopic dipoles generated at the layer boundaries by arranging the dipoles in an alternately antiparallel manner.[16] These two models indicated that control of the large dipoles at the boundaries was important for generation of the Sm-C_A phases. On the other hand, swallow-tail liquid crystalline compounds without an asymmetric carbon atom also exhibited Sm-

(8) (a) Suzuki, Y.; Isozaki, T.; Hashimoto, S.; Kusumoto, T.; Hiyama, T.; Takanishi, Y.; Takezoe, H.; Fukuda, A. *J. Mater. Chem.* **1996**, *6*, 753. (b) Jin, B.; Ling, Z.; Takanishi, Y.; Ishikawa, K.; Takezoe, H.; Fukuda, A.; Kakimoto, M.; Kitazume, T. *Phys. Rev. E* **1996**, *53*, R4295. (c) Ouchi, Y.; Yoshioka, Y.; Ishii, H.; Seki, K.; Kitamura, M.; Noyori, R.; Takanishi, Y.; Nishiyama, I. *J. Mater. Chem.* **1995**, *5*, 2297. (d) Kusumoto, T.; Isozaki, T.; Suzuki, Y.; Takanishi, Y.; Takezoe, H.; Fukuda, A.; Hiyama, T. *Jpn. J. Appl. Phys.* **1995**, *34*, L830. (e) Hori, K.; Endo, K. *Bull. Chem. Soc. Jpn.* **1993**, *66*, 46. (f) Cladis, P. E.; Bland, H. R. *Liq. Cryst.* **1993**, *14*, 1327. (g) Bland, H. R.; Cladis, P. E.; Pleiner, H. *Macromolecules* **1992**, *25*, 7223.

(9) (a) Miyachi, K.; Fukuda, A. Antiferroelectric Liquid Crystals. In *Handbook of Liquid Crystals: Low Molecular Weight Liquid Crystals II*; Demus, D., Goodby, J., Gray, G. W., Spiess, H.-W., Vill, V., Eds.; Wiley-VCH: Weinheim, 1998; Vol. 2B, Chapter 4, pp 665−691. (b) Nishiyama, I. *Adv. Mater.* **1994**, *6*, 996. (c) Fukuda, A.; Takanishi, Y.; Isozaki, T.; Ishikawa, K.; Takezoe, H. *J. Mater. Chem.* **1994**, *4*, 997. (d) Goodby, J. W. *J. Mater. Chem.* **1991**, *1*, 307.

(10) Gorecka, E.; Nakata, M.; Mieczkowski, J.; Takanishi, Y.; Ishikawa, K.; Watanabe, J.; Takezoe, H.; Eichhorn, S. H.; Swager, T. M. *Phys. Rev. Lett.* **2000**, *85*, 2526.

(11) Gorecka, E.; Čepič, M.; Nakata, M.; Takezoe, H.; Žekš, B. *Book of Abstracts, 19th International Liquid Crystal Conference 2002*, C4, Edinburgh, UK.

(12) Thisayukta, J.; Samulski, E. T. *Book of Abstracts, 19th International Liquid Crystal Conference 2002*, C79, Edinburgh, UK.

(13) Pratibha, R.; Madhusudana, N. V.; Sadashiva, B. K. *Science* **2000**, *288*, 2184.

(14) Maiti, P. K.; Lansac, Y.; Glaser, M. A.; Clark, N. A. *Condensed Mater.* **2001**, 0107558v1.

(15) Takanishi, Y.; Hiraoka, K.; Agrawal, V. K.; Takezoe, H.; Fukuda, A.; Matsushita, M. *Jpn. J. Appl. Phys.* **1991**, *30*, 2023.

(16) Miyachi, K.; Matsushima, J.; Takanishi, Y.; Ishikawa, K.; Takezoe, H.; Fukuda, A. *Phys. Rev. E* **1995**, *52*, R2158.

Scheme 3. Schematic Side View of the Layer Structure in a Smectic C_A Phase Induced by Doping

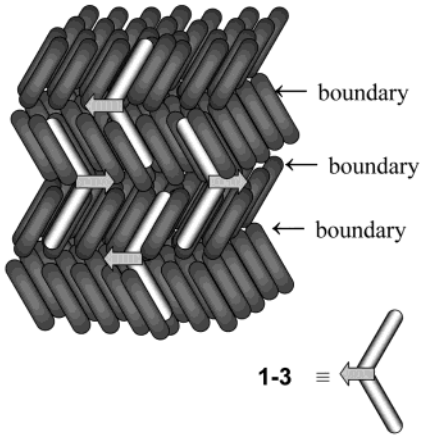

C_A phases, and the forked alkyl chain was assumed to be important for generation of the phase.[17] It appeared that interdigitation of the alkyl chains between the layers controlled the relation between the tilt directions in the adjacent two layers. This suggested that the steric interlayer interaction was also important for generation of the Sm-C_A phase.

Result and Discussion

Design of the Dopant. We thought that a Sm-C_A phase could be induced from a Sm-*C* phase by suspending dopant molecules **1**−**3** at the boundaries as shown in Scheme 3. Compounds **1**−**3** have the following features: (1) a long bent-core molecule which has one carbon atom as the linkage of the two long straight rods; if a small amount of the dopant molecules is added to a Sm-*C* phase of rodlike molecules, the central parts of the bent-core molecules are moved out of the layers of the straight cores and suspended at the boundaries of the layers; and (2) a central strong dipole generated by a $-C(CF_3)_2-$ linkage group; the central parts aggregated at the boundaries generate the large macroscopic dipoles. The macroscopic dipoles are alternately arranged from boundary to boundary to cancel out themselves. From previous reports,[18] it was expected that the large lateral dipole at the molecular center was effective to generate highly ordered organization in the liquid crystal phases.

Behavior of the Dopant Molecules. Behavior of the dopant molecules is shown in Table 1. Compounds **1** and **2** did not exhibit any liquid crystal phase. Compounds **3a**−**c** exhibited stable enantiotropic liquid crystal phases as smectic X (Sm-*X*) phases (Figure 1). It was very difficult to find the homeotropic or Schlieren textures in the mesophases. In the Sm-*X* phase, the fanlike and batonet textures had dark shadow lines parallel to the directions of the crossed polarizers in polarized light optical microscopy, which meant that their optic axes were perpendicular to the layer planes. However, Schlieren or homeotropic textures could not be observed even after chemical coating of the glass surface using hexamethyldisilazane. From these observations, we could not determine the layer structure of the phase.

Table 1. Behavior of Compounds 1−3

compound	behavior[a]
1	Cr $\underset{77\ (-13.0)}{\overset{106\ (17.1)}{\rightleftharpoons}}$ I
2	Cr1 $\underset{100\ (-0.3)}{\overset{102\ (0.3)}{\rightleftharpoons}}$ Cr2 $\underset{114\ (-4.1)}{\overset{123\ (4.2)}{\rightleftharpoons}}$ I
3a	Cr $\underset{181\ (-3.5)}{\overset{223\ (3.9)}{\rightleftharpoons}}$ SmX $\underset{276\ (-4.4)}{\overset{283\ (4.5)}{\rightleftharpoons}}$ I
3b	Cr1 $\underset{181(-5.3)}{\overset{186(3.1)}{\rightleftharpoons}}$ Cr2 $\underset{184\ (-2.7)}{\overset{196\ (3.5)}{\rightleftharpoons}}$ SmX $\underset{252\ (-6.3)}{\overset{256\ (6.7)}{\rightleftharpoons}}$ I
3c	Cr $\underset{149\ (-4.9)}{\overset{165\ (4.4)}{\rightleftharpoons}}$ SmX $\underset{202\ (-5.1)}{\overset{205\ (5.0)}{\rightleftharpoons}}$ I

[a] The transition temperatures (°C) and enthalpies (in parentheses, kcal/mol) were determined by DSC (5 °C/min) and are given above and below the arrows. Cr, Cr1, and Cr2 indicate crystal phases. N, and I indicate nematic and isotropic phases, respectively. SmX indicates a smectic phase unidentified.

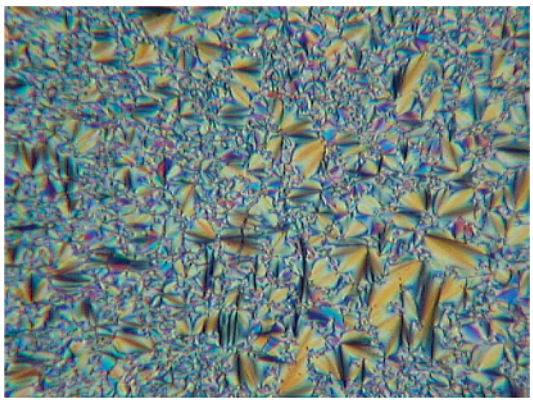

Figure 1. Polarized light micrograph of **3c** in the smectic X phase (cross-polarization position, at 200 °C, ×400).

XRD Experiments of Mesophases of 3a−c. To investigate molecular packing structure in the Sm-*X* phase, an XRD experiment was performed. The layer distances (*d*) of **3a**−**c** were observed at 25.7, 27.8, and 32.0 Å, respectively, and those halos were observed at 4.8−4.9 Å. The peaks in the small angle regions were small and broad like those of nematic phases, which indicated that the phases had highly disordered packing structures. Each of the layer distances was shorter than the corresponding half molecular length. The length from the center to the end of the terminal chain (*l*′) was estimated from MM2 calculation[19] for each compound (**3a**, 31; **3b**, 34; and **3c**, 38 Å), and arccosine of the *d*/*l*′ was calculated to give the tilt angle θ (**3a**, 34; **3b**, 34; and **3c**, 33°). Considering the bent angle of the core (ca.

(17) Nishiyama, I.; Goodby, J. W. *J. Mater. Chem.* **1993**, *3*, 149.
(18) (a) Kishikawa, K.; Furusawa, S.; Yamaki, T.; Kohmoto, S.; Yamamoto, M.; Yamaguchi, K. *J. Am. Chem. Soc.* **2002**, *124*, 1597. (b) Eichhorn, S. H.; Paraskos, A. J.; Kishikawa, K.; Swager, T. M. *J. Am. Chem. Soc.* **2002**, *124*, 12742. (c) Levitsky, I. A.; Kishikawa, K.; Eichhorn, S. H.; Swager, T. M. *J. Am. Chem. Soc.* **2000**, *122*, 2474. (d) Kishikawa, K.; Harris, M. C.; Swager, T. M. *Chem. Mater.* **1999**, *11*, 867.

(19) MM2 calculation: molecular modeling of compounds **1** and **2** was carried out by ChemBats3D (Cambridge Software Corporation).

Scheme 4. Schematic Side View of the Layer Structure in the Sm-*X* Phase of 3

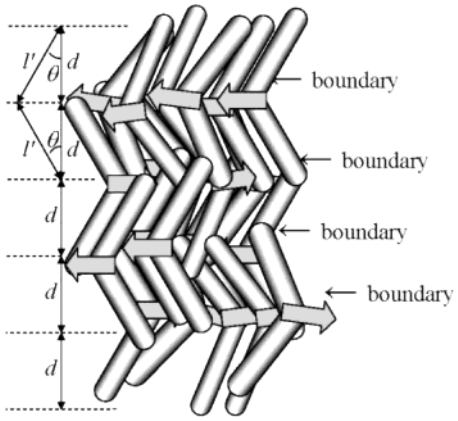

110°), these tilt angles indicated that the molecular long axes were almost parallel to the layer normal. From the XRD data, the dipole−dipole interaction, and the molecular shape, the packing diagram of the Sm-*X* phase was postulated as shown in Scheme 4.The molecules seem to be arranged in an alternately antiparallel manner in the direction of the layer normal to cancel out their dipoles.

Miscibility Experiment of 1 and 3c. A miscibility experiment of **1** and **3c** (Figure 2) was performed to confirm the similarity in their packing structures. Pure **1** did not exhibit any liquid crystal phase. However, the monotropic Sm-*X* phase was generated by doping with 10 wt % of **3c** and the enantiotropic Sm-*X* phase was generated by doping with 20 wt % of **3c**. The temperature range of the Sm-*X* phase was almost constant at 20−100 wt %. From this experiment, it was confirmed that bent-core molecules **1** and **3c** were freely miscible in the liquid crystal phases, and this meant that each of the mixtures had similar packing structures in the content range of 10−100 wt % of them. Accordingly, the packing structure of **1** in the crystal phase was assumed to be similar to that of **3c** in the liquid crystal phase as shown in Scheme 4.

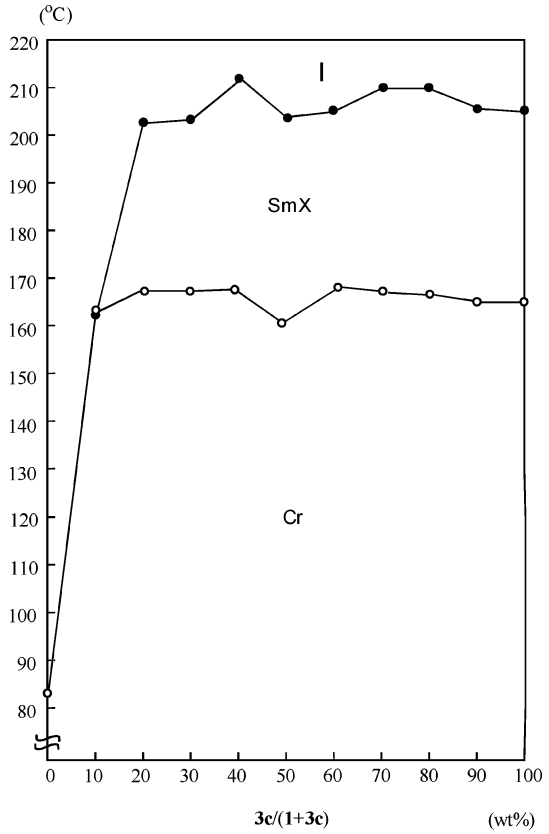

Figure 2. Miscibility experiment of **1** and **3c**. The transition temperatures were plotted. I, isotropic liquid; SmX, smectic X phase (unidentified smectic phase); Cr, crystal.

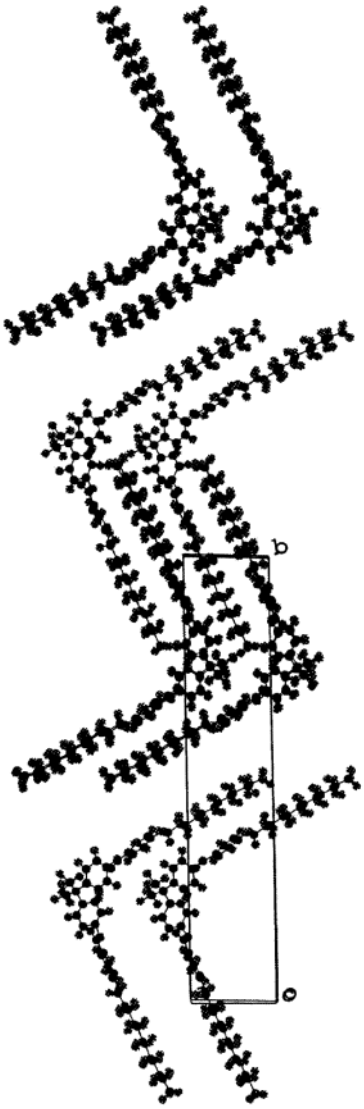

Figure 3. Packing structure of **1** in the crystal phase.

Single-Crystal X-ray of 1. Though the single crystals of **2** and **3** were not obtained, those of **1** were obtained by recrystallization from hexane−chloroform. To investigate the packing structure of **1**, X-ray diffraction of the single crystal was measured, and the crystal structure was solved (Figure 3). The bent molecules are organized in each layer in a parallel manner, and the molecules are piled up in an alternately antiparallel manner with every shift of the half molecular length with respect to the layer normal. It is almost similar to the packing structure of **3** shown in Scheme 4.

From miscibility experiments of **1** and **3c** and the single-crystal X-ray crystallography of **1**, the packing structures of **3** in the liquid crystal phase were strongly assumed to have the antiparallel layer structures as postulated in Scheme 4.

Scheme 5. Liquid Crystalline Compounds 4−7 Which Have Smectic C Phases; Phase Transitions Are in Parentheses

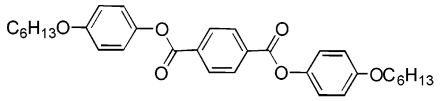

4 (Cr 162 Sm-C 178 Sm-A 182 N 208 I)

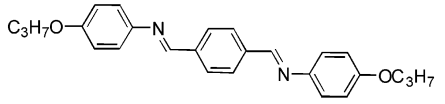

5 (Cr 109 Sm-H 115 Sm-G 143 Sm-C 154 Sm-A 181 N 255 I)

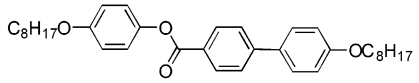

6 (Cr 120 (Sm-X 118) Sm-C 162 Sm-A 200 N 202 I)

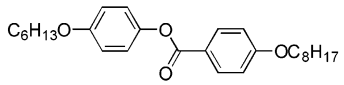

7 (Cr 37 Sm-C 55 N 81 I)

Table 2. Combination of a Dopant and a Mother Liquid Crystalline Compound, and the Minimum Amount of Dopants for Induction of a Smectic C_A Phase

entry	dopant	mother liquid crystalline compound	minimum amount of dopants for induction of a smectic C_A[a] (wt%)
1	**1**	**4**	*b*
2	**1**	**5**	*b*
3	**1**	**6**	*b*
4	**1**	**7**	5
5	**2**	**4**	5
6	**2**	**5**	10
7	**2**	**6**	2
8	**2**	**7**	2[c]
9	**3c**	**4**	1
10	**3c**	**5**	5
11	**3c**	**6**	2
12	**3c**	**7**	5[c]

[a] In the miscible experiments, 0.1, 1, 2, 5, 10, and 20 wt % of dopants were added and the textures were observed by polarized optical microscopy. [b] The smectic C_A phase was not observed. [c] The smectic C_A phase was observed with a nematic phase.

Miscibility Experiment of the Dopants and Liquid-Crystalline Compounds 4−7. To know the best combination of a dopant and a liquid crystalline compound, dopants **1**−**3** were mixed with known liquid crystalline compounds **4**−**7** (Scheme 5) which exhibit a Sm-*C* phase. The minimum amounts of the dopant for induction of the Sm-C_A phase are shown in Table 2. The Sm-C_A phases were identified by polarized light microscopy in which the two- and six-brushes in the Schlieren textures (Figure 4) were observed. All of *N*, Sm-*C*, and Sm-C_A phases exhibit Schlieren textures. However, the defects of each phase are quite different from those of the other phases and indicative of its own topology around the defect. The Schlieren textures of Sm-*C* phases have only 4-brush defects and cannot have 2-brush defects (Figure 5, upper). The synclinic tilting of the molecules in the layers does not generate discontinuous defect planes which are observed as 2-brush defects. The Schlieren textures of *N* phases have both

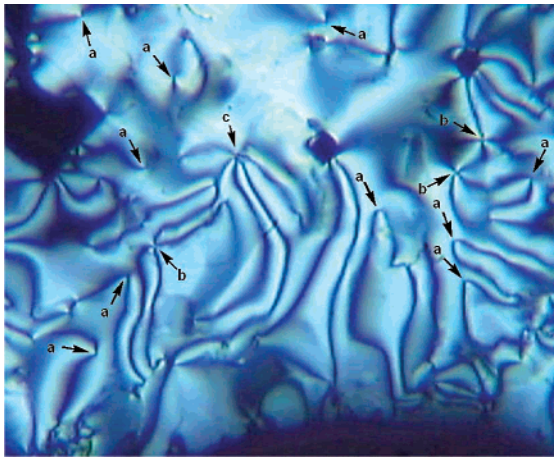

Figure 4. Polarized optical micrograph of a mixture of **4** and **3** (70:30). The Schlieren texture had the two- (a), four- (b), and six-brushes (c) (180 °C, ×400).

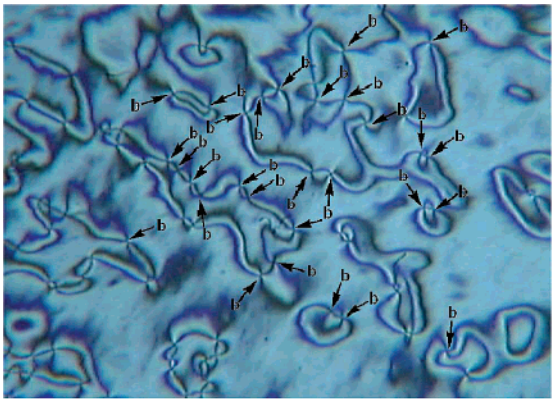

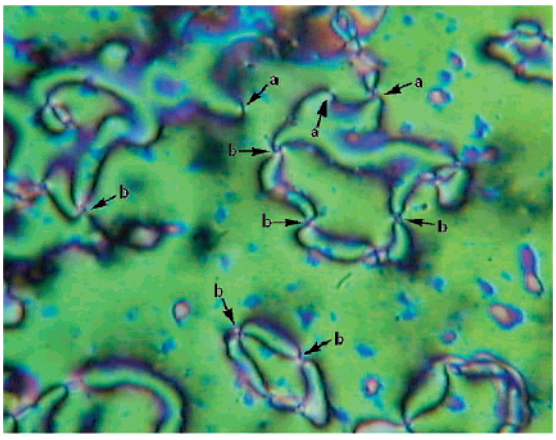

Figure 5. Polarized optical micrographs of **4** in the smectic C (upper) and nematic (lower) phases. The smectic C phase had only four-brushes (b) (170 °C, ×400), and the nematic phase had both two- (a) and four-brushes (b) (200 °C, ×400).

2- and 4-brush defects (Figure 5, lower), because they can generate the discontinuous defect planes. On the other hand, the Schlieren textures of Sm-C_A phases have all of 2-, 4-, and 6-brushes because of the anticlinic tilting of the molecules in the layers, which was explained by Takanishi et al.[20,21] They concluded that

(20) (a) Takanishi, Y.; Takezoe, H.; Fukuda, A.; Watanabe, J. *Phys. Rev.* **1992**, *B45*, 7684. (b) Takanishi, Y.; Takezoe, H.; Fukuda, A.; Komura, H.; Watanabe, J. *J. Mater. Chem.* **1992**, *2*, 71.

(21) Takanishi, Y.; Takezoe, H.; Fukuda, A. *Ferroelectrics* **1993**, *149*, 133.

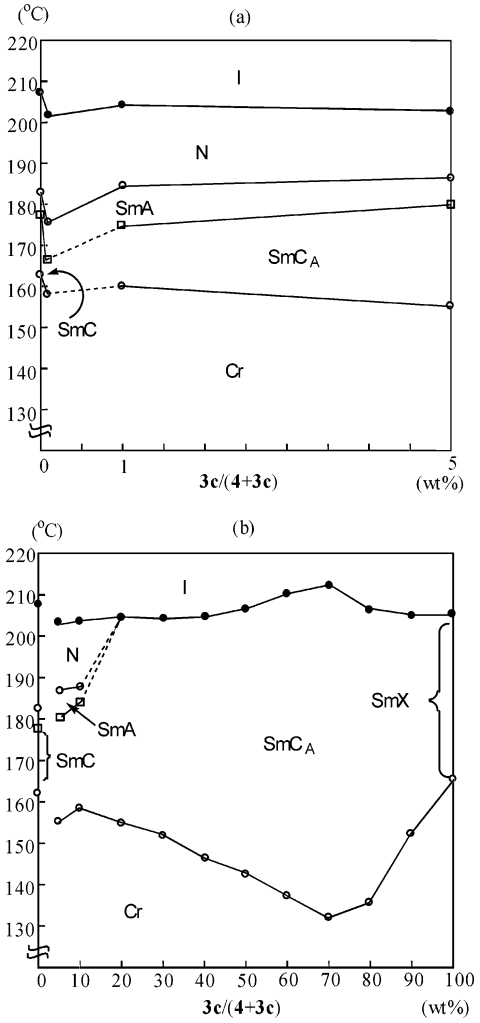

Figure 6. Miscibility experiment of **4** and **3c**. The transition temperatures were plotted. I, isotropic liquid; SmA, smectic A phase; SmC, smectic C phase; SmC_A, smectic C_A phase; Cr, crystal; SmX, unidentified smectic phase. The charts are depicted in ranges of (a) 0−5 wt % and (b) 0−100 wt % of **3c**/(**4** + **3c**), respectively.

both of the 2- and 6-brushes originated in wedge-screw dispirations.

Accordingly, existence of both 2- and 6-brushes in the Schlieren textures is indicative of the phase being a Sm-C_A phase. Further, the dark lines in the fanlike texture and the carved domains were parallel to either the polarizer or the analyzer of the polarized light microscope, which meant that the optic axes averaged were perpendicular to the layer planes and that the phase was a Sm-C_A phase not a Sm-*C* phase. Compounds **4**, **5**, and **6** did not exhibit Sm-C_A phases by addition of **1** at the contents of 0.1−20 wt %. The other entries show that Sm-C_A phases are generated by addition of 1−10 wt % of the dopants. The smallest dopant percentage in this series (1 wt %) was achieved in the combination of compound **4** and dopant **3c**.

The miscibility experiment of **4** and **3c** was carried out in the range of 0−100 wt % (Figure 6). The nematic and Sm-*A* phases disappeared in the range over 20 wt % of the dopant and only the Sm-C_A phase was observed. At 70 wt % of **3c**, the Sm-C_A phase had the broadest temperature range in this experiment, and the molar ratio of **4**/**3c** was ca. 2:1 which might generate the most stable packing structure in the mesophase.

Table 3. Half-Molecular Lengths and Half-Core Lengths of 1, 2, and 3c, and the Molecular Lengths, Core Lengths, and Dipole Moments of 4−7

compound	molecular length (Å)	core length (Å)	molecular dipole moment (debye)
1	29[a]	11[b]	
2	35[a]	17[b]	
3c	38[a]	20[b]	
4	36[c]	17[d]	0.0[e]
5	29[c]	17[d]	0.0[e]
6	39[c]	14[d]	3.2[e]
7	32[c]	11[d]	2.8[e]

[a] Distance from the central carbon-atom possessing two CF_3 groups to the end of the alkyl chain. [b] Distance between the carbon atom at 1-position of the 2-phenyl group and the carbon atom possessing the terminal alkoxy group. [c] Distance between the two carbon atoms possessing the terminal alkoxy group. [d] Distance between the carbon atoms of the two benzene rings possessing the terminal alkoxy group. [e] The dipole moments were calculated by AM1 (ref 22).

Investigation of the Structural Difference Between the Matched and Mismatched Pairs. We attempted explanation of the structural difference between the matched and mismatched pairs. First, dipole−dipole interaction between the dopants and the liquid-crystalline molecules was investigated. Dopants **1**−**3** have a 1,1,1,3,3,3-hexafluoro-2,2-diphenylpropane moiety at the center in which the lateral dipole is 3.9 D in AM1 calculation,[22] and the two straight rodlike wings have the ester linkages which have a dipole along each of the wings. On the other hand, the dipole moments of liquid-crystal molecules **4**, **5**, **6**, and **7** were 0, 0, 3.2, and 2.8 D, respectively (Table 3). It was expected that the polar molecules (**6** and **7**) have larger dipole−dipole interaction with the dopants than the nonpolar molecules (**4** and **5**). However, effect of those molecular dipoles was not clear in the miscibility experiment (Table 2). Therefore, the molecular lengths and the core lengths were calculated by MM2 molecular modeling.[22] The molecular lengths/core lengths of **4**−**7** were 36/17, 29/17, 39/14, and 32/11 Å, respectively, as shown in Table 3, and the half molecular lengths/core lengths of **1**, **2**, and **3c** were 29/11, 35/17, and 38/20 Å, respectively, as shown in Table 3. In the cases of **4**, **5**, and **6**, the longer dopant induced a *Sm*-C_A phase with the smaller ratio of the dopant, because of the attractive core−core interaction with the liquid crystal molecules. Moreover, the shortest dopant (**1**) induced the Sm-C_A phase specifically with **7** which has the shortest core-length in this series. However, **1** did not induce a Sm-C_A phase in the cases of **4**−**6**. This meant that matching in the core-lengths is also an important factor for the induction.

Investigation of Effect of the Central Dipole of the Dopants. To investigate effect of the central dipole of the dopants on stability of the mesophase, the phase behavior of **7** doped with **1** (X = CF_3) was compared with that of **7** doped with **1′** (X = CH_3), as shown in Figure 7a and b. The Nematic, Sm-*A*, Sm-*C*, and Sm-C_A phases were identified by observation of their textures in polarized light optical microscopy. To our surprise, addition of these dopants was effective to raise the

(22) AM1 calculation was carried out by WinMOPAC Ver. 3 (Fujitsu, Ltd.). Stewart, J. J. P. *J. Comput. Chem.* **1989**, *10*, 209−220 and 221−264.

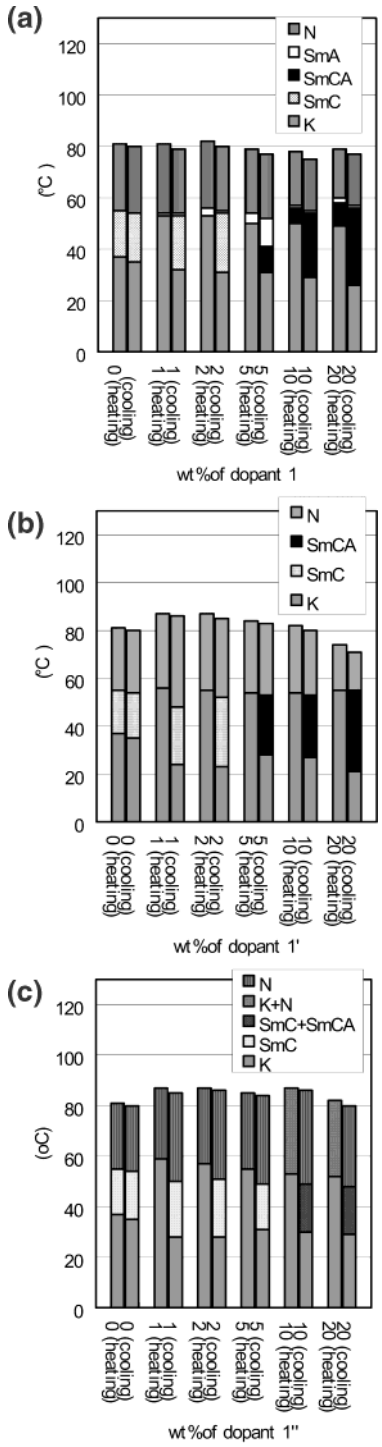

Figure 7. Bar graphs showing the phase behavior of **7** doped with (a) **1** (X = CF_3), (b) **1′** (X = CH_3), and (c) **1″** (X = H) on heating and cooling (rate, 1 °C/min). The temperature ranges are drawn against wt % of the dopant. N, SmA, SmCA, SmC, and K indicate nematic, smectic A, smectic C_A, smectic C, and crystal phases, respectively. K + N indicates a phase consisting of both crystal and nematic phases. SmC + SmCA indicates a liquid crystal phase consisting of both smectic C and smectic C_A phases.

melting points in the range of 1−20% contents. In both the cases, **7** exhibited both Sm-*C* and Sm-C_A phases at the dopant ratios of 1−2 wt % and 5−20 wt %, respectively. Compound **7** doped with **1** exhibited enantiotropic Sm-C_A phases at 10−20 wt % of the dopant with decrease of the melting points. However, in the case of **7** doped with **1′**, the melting points were almost constant in the dopant range of 1−20 wt %, and enantiotropic Sm-C_A phases could not be obtained. Accordingly, it is obvious that addition of **1** (X = CF_3) is more effective to stabilize the layer structure of Sm-C_A phases than that of **1′** (X = CH_3).

This difference originates in the electrostatic difference between molecules **1** and **1′** because the size of CF_3 is almost the same as that of CH_3. It is assumed that the macroscopic dipole generated by the dopant molecules at the layer boundaries stabilizes the layer structure of the Sm-C_A phases as shown in Scheme 3. Then, to investigate the spatial effect of the central linkages of **1** and **1′**, the miscibility experiment of **7** with **1″** (X = H) was performed (Figure 7c). At 1−5 wt % of the dopant, enantiotropic nematic phases were also observed. However, at 10−20 wt %, the solid remained on heating in the temperature range of the nematic phase, and in the temperature range of the Sm-C_A phase the domains exhibiting the Sm-*C* phase were observed in polarized light optical microscopy. This indicated that dopant **1″** had not been dispersed homogeneously in **7**. Accordingly, it was assumed that introduction of CF_3 (or CH_3) at the molecular center was effective to improve the dispersion ability of the dopants.

Conclusion

The following information were obtained in this study. (1) The transformation by doping with a small amount of dopant indicated that the energy gaps between the Sm-*C* and Sm-C_A phases are very small. (2) Steric interaction of the bent-core molecules with the rodlike molecules at the boundary was important for induction of a Sm-C_A phases. (3) Matching of the core lengths between the dopant and the liquid crystalline molecules was important for the effective induction. (4) The macroscopic dipoles at the boundaries played an important role for stabilization of a Sm-C_A phase. The most dominant factor for induction of a Sm-C_A phase seemed to be that the dopant had a bent-rod shape, because Sm-C_A phases were obtained in the cases of both the short dopant (**1**) and the nonpolar dopant (**1″**). The other factors, matching of core lengths and the central dipole, were effective to stabilize the Sm-C_A phases induced. From this study, it is expected that most Sm-*C* phases can be changed into the corresponding Sm-C_A phases by doping with our dopants, and it may accelerate development of antiferroelectric (Sm-C_A*) LCDs.

Acknowledgment. This work was supported by Izumi Science and Technology Foundation, Iketani Science and Technology Foundation, and a Grant-in-Aid for Scientific Research (C) from the Japan Society for the Promotion of Science (JSPS) (13640571). We thank Chiba University Radioisotope Research Center for measurement of powder X-ray diffraction of the liquid crystals.

Supporting Information Available: Synthesis of dopants (**1**, **1′**, **1″**, **2**, **3a**, **3b**, and **3c**), crystal data of **1**, and XRD of **3a**, **3b**, and **3c** (PDF; 9 pages). These materials are available free of charge via the Internet at http://pubs.acs.org.

CM0340476